Materials and Energy Research Center
MERC

Contents lists available at ACERP

Advanced Ceramics Progress

Journal Homepage: www.acerp.ir

Original Research Article

Synthesis of Zinc Sulfide (ZnS) Nano-powder by Chemical Method

Ali Sedaghat Ahangari Hossein Zadeh [a,*], Mohammad Zakeri [a]

[a] *Associate Professor, Division Department of Ceramics, Materials and Energy Research Center, Karaj, Iran.*

* Corresponding Author Email: a.sedaghat@merc.ac.ir (A. Sedaghat Ahangari Hossein Zadeh) URL: https://www.acerp.ir/article_244714.html

ARTICLE INFO

Article History:
Received 06 May 2026
Revised 23 May 2026
Accepted 26 May 2026

Keywords:
Synthesis,
Zinc Sulfide,
Nano-Powder,
Chemical Method

ABSTRACT

This study explores the synthesis and characterization of zinc sulfide (ZnS) nanostructured powder using a chemical method. The research systematically evaluates the effects of critical synthesis parameters, such as the mass ratio of the sulfide precursor to the zinc precursor, the pH of the solution, and the synthesis temperature. The resulting ZnS samples were extensively characterized using a variety of analytical techniques, including X-ray diffraction (XRD), Fourier-transform infrared (FTIR) spectroscopy, field emission scanning electron microscopy (FESEM), energy-dispersive X-ray spectroscopy (EDS), and dynamic light scattering (Zetasizer) analysis. The results of the study revealed that the ZnS powder produced at a pH of 1.2, referred to as ZnS4, exhibited an average particle size of 31 nm, which is considerably smaller than that of the other synthesized nanopowders. FTIR spectroscopy confirmed the high purity of ZnS4, indicating a lower absorption edge and diminished levels of impurities compared to the other synthesized samples. Furthermore, the sintered ZnS4 sample demonstrated an infrared transmittance of approximately 30% within the wavelength range of 8–12 micrometers. This finding underscores the potential of ZnS4 as a viable candidate for applications in infrared optics, including infrared windows and coatings.

https://doi.org/10.30501/acp.2026.580678.1194

1. INTRODUCTION

Zinc sulfide (ZnS) is extensively studied as a semiconductor material, recognized for its superior optical and chemical characteristics, particularly its high transparency in the infrared (IR) spectrum. The material's substantial energy bandgap, ranging from 3.72 to 3.77 eV, results in minimal absorption within the 8–12 µm wavelength range, rendering it suitable for various IR applications, such as IR windows, missile domes, lasers, and optoelectronic devices [Ramavath et al., 2014– Yeo, 2018]. ZnS can crystallize in two predominant structures, sphalerite (cubic) and wurtzite (hexagonal). The cubic structure is more thermodynamically stable under standard conditions and is favored for optical applications due to its enhanced transparency. Conversely, the hexagonal wurtzite phase, which may form at elevated temperatures, can significantly impair IR transmittance due to phenomena such as birefringence and scattering [Chen, 2015]. Notwithstanding its promising capabilities, the expense associated with the fabrication of high-quality ZnS infrared windows continues to pose a considerable obstacle to their broader implementation. This challenge arises from the intricate manufacturing processes necessary to attain the requisite transparency while simultaneously minimizing the occurrence of the undesirable hexagonal phase.

At present, the production of ZnS is primarily dominated by two methods, chemical vapor deposition

Please cite this article as: Sedaghat Ahangari Hossein Zadeh, A., & Zakeri,, M. (2025). Synthesis of Zinc Sulfide (ZnS) Nano-powder by Chemical Method to improve its Optical Properties. *Advanced Ceramics Progress*, *11*(3), 31-38. https://doi.org/10.30501/acp.2026.580678.1194

(CVD) and hot-press (HP) sintering. CVD is particularly effective for the fabrication of large, transparent polycrystalline ZnS window plates; however, it is associated with high costs, extended processing times, and suboptimal mechanical properties. Conversely, HP sintering offers enhanced mechanical strength and reduced production durations, yet it necessitates elevated temperatures exceeding 950°C, which approach the phase transition temperature of ZnS (1020°C), thereby posing risks of structural instability. Furthermore, HP sintering entails a prolonged processing cycle that typically exceeds ten hours [Li, 2016; Ramavath, 2011].

Historically, hot pressing (HP) has been employed in the fabrication of infrared-transparent ZnS ceramics; however, its inherent limitations have prompted the exploration of vacuum hot pressing (VHP) as a viable alternative. VHP has demonstrated promise in the production of transparent ZnS ceramics, exhibiting enhanced properties that effectively balance optical transparency and mechanical strength, while also mitigating the shortcomings associated with traditional fabrication techniques [Drezner, 2001; Yashina, 2004].

Hybrid methodologies that integrate wet chemistry for the synthesis of nanoparticles with solid-state sintering present a compelling alternative in materials production [Sharma, 2023]. Wet chemistry approaches, particularly those that emphasize the generation of monodisperse nanoparticles, provide advantages in scalability and uniform particle homogeneity, which are essential for industrial applications. The subsequent sintering process can be conducted using conventional HP methods or more advanced techniques such as spark plasma sintering (SPS). SPS is advantageous due to its ability to operate at lower sintering temperatures [Abedi, 2023] and reduced processing durations compared to traditional HP, thereby allowing for enhanced control over microstructural characteristics and, consequently, improvement of material properties. The overarching goal in optimizing ZnS production is to establish methodologies that reduce both production costs and time while simultaneously enhancing transparency and mechanical strength. Hybrid approaches that incorporate advanced sintering techniques, such as SPS, show significant potential for addressing current limitations and producing high-quality ZnS materials suitable for demanding applications.

This research explores the synthesis and characterization of ZnS nanoparticles through a wet chemical approach. A systematic analysis was conducted to assess the impact of critical reaction parameters on the production of ZnS nanoparticles. Following synthesis, the ZnS nanoparticles were subjected to sintering via the SPS technique, and their optical properties were subsequently analyzed.

2. MATERIALS AND METHODS

2.1. Reagents and materials

All chemicals mentioned in the experiment were of analytical grade and deionized water used for preparation of chemical solutions in our experiments.

2.2. Characterization

The morphologies of the ZnS nanopowder samples and sintered ZnS were investigated using field emission scanning electron microscopy (FESEM) in conjunction with energy-dispersive X-ray spectroscopy (EDS) to determine the elemental composition. The crystalline structure of the material was evaluated through XRD patterns, which were analyzed using a D8 ADVANCE X-ray diffractometer (Bruker, Germany) with Cu-Kα radiation (λ = 1.54 Å). The characteristics of the ZnS powders in the range of 400–4000 cm^{-1}, as well as the optical transmission spectra of the samples spanning 1.2–20 μm, were obtained via FTIR spectroscopy using a Vector 33 FTIR spectrometer (Bruker, Germany). Additionally, the size of the ZnS nanoparticles was measured using an HS 3000 Zetasizer (Malvern, United Kingdom).

2.3. Preparation of zinc sulfide nano-powder samples

Zinc sulfide was synthesized using a precipitation method, employing 62.65 g of sodium sulfide (Na_2S) and 52.60 g of zinc acetate ($Zn(CH_3COO)_2$). Both precursor compounds were dissolved in 450 mL of deionized water and subjected to sonication for 30 minutes. The pH of the zinc acetate solution was subsequently adjusted to 4.0 using hydrochloric acid. The zinc acetate solution was then heated to 75 °C under an argon atmosphere, after which the sodium sulfide solution was added dropwise over a period of 30 minutes, resulting in the formation of a milky suspension. The reaction mixture was maintained at 60 °C for 10 hours to ensure complete precipitation. The resulting ZnS precipitate was isolated via gravity filtration and thoroughly washed with deionized water, acetone, ethanol, and deionized water again over a period of 7 hours. The solid product was dried at 65 °C, ground, and subsequently sieved through a 60-mesh sieve.

This study aimed to optimize the synthesis of ZnS powder to improve its optical properties. The effects of varying the weight ratio of Na_2S to zinc acetate ($Zn(CH_3COO)_2$), as well as pH and reaction temperature, were investigated. For analytical purposes, the synthesized samples were assigned codes corresponding to their respective synthesis conditions, as detailed in Table 1.

The ZnS powder deemed most appropriate based on a comprehensive evaluation of its properties was subjected to sintering using a spark plasma sintering apparatus to enhance its mechanical properties.

Table 1. ZnS samples and their synthesis conditions

Temperature (°C)	pH	Na_2S:$Zn(CH_3COO)_2$	Sample code
80	4	1.19:1	ZnS1
80	4	1:1	ZnS2
80	4	2:1	ZnS3
80	1.2	1.19:1	ZnS4
80	5	1.19:1	ZnS5
50	4	1.19:1	ZnS6
110	4	1.19:1	ZnS7

2.4. Sintering process

The untreated powders were placed into a graphite mold with a punch diameter of 30 mm. Prior to the sintering process, a uniaxial pressure of 20 MPa was applied after loading the sample. Subsequently, the applied pressure was incrementally increased to a maximum of 80 MPa over a period of 15 minutes, coinciding with the sintering temperature reaching 750 °C. The ZnS ceramics produced via spark plasma sintering were then subjected to mirror polishing on both surfaces using 800, 1000, and 2000 mesh abrasive papers in a sequential three-step procedure.

3. RESULTS AND DISCUSSION

3.1. Characterizations of ZnS nano-powders samples

Figure 1 presents the XRD patterns of the synthesized ZnS nanopowder samples. The diffraction peaks across all samples exhibit a high degree of similarity, primarily aligning with the sphalerite structure, as corroborated by standard card No. 96-500-0089, which indicates a cubic crystal structure. While it is possible that trace impurities, such as carbon or elemental sulfur, exist at concentrations below 0.5%, the observed peak broadening and reduced intensities strongly suggest that the synthesized ZnS particles are in the nanoscale range. The crystallite size for each sample was calculated using the Scherrer equation, and the results are summarized in Table 2. Notably, among the samples analyzed, ZnS5 exhibited the largest crystallite size, whereas ZnS2 demonstrated the smallest.

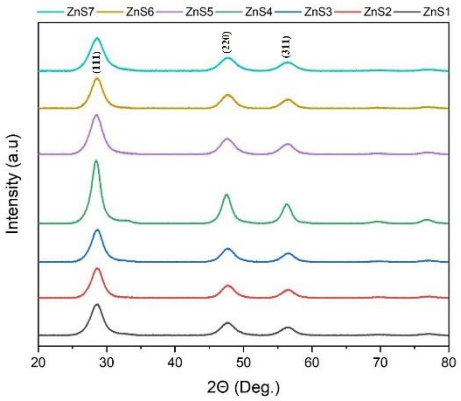

Figure 1. X-ray diffraction patterns of ZnS nano-powders

Table 2. Crystallite size of synthesized ZnS samples

Sample	Crystallite size (Å)
ZnS1	37
ZnS2	42
ZnS3	41
ZnS4	31
ZnS5	47
ZnS6	41
ZnS7	39

The FTIR spectra show the characteristic Zn–S stretching vibrations, which have been reported in the literature [Rema, 2007; Zahabi, 2024] over a range from approximately 480 to 670 cm^{-1}. In the present work, the band at 670 cm^{-1} is assigned to the Zn–S stretching mode. The main peaks (O–H stretching at 3450 cm^{-1}, O–H bending at 1630 cm^{-1}, the 980 cm^{-1} band, and the 670 cm^{-1} Zn–S band) are now indicated directly on the spectrum in Figure 2 for clarity.

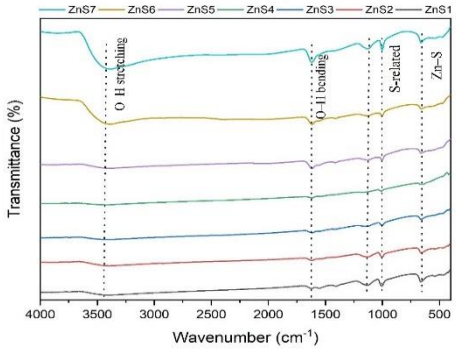

Figure 2. FTIR spectra of ZnS nano-powders

Figures 3 and 4 illustrate the FESEM and EDS images of ZnS nanoparticles. The surface morphology of all examined samples predominantly exhibits a spherical shape, indicative of relatively uniform particle

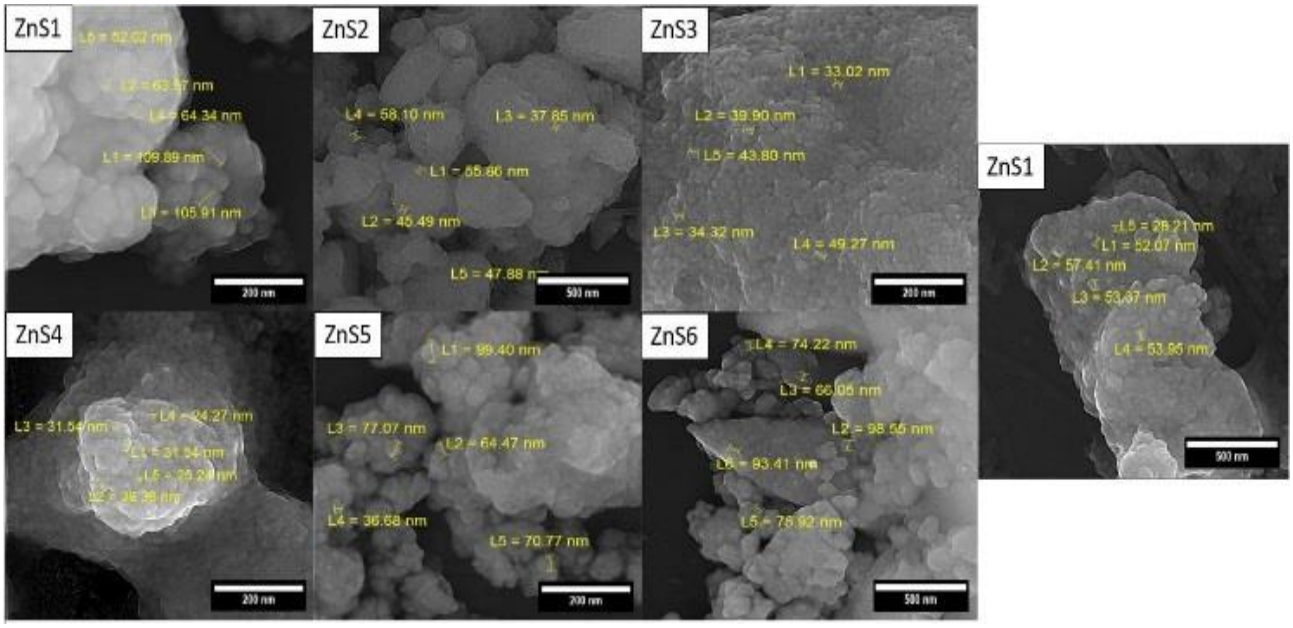

Figure 3. FESEM images of ZnS nano-powders

characteristics, which is a hallmark of well-structured nanomaterials. The ZnS particles across all samples are confirmed to be nanosized, falling within the typical nanoparticle size range, and are observed in the form of agglomerates. This aggregation phenomenon can be attributed to van der Waals forces and interparticle interactions, which are commonly observed in nanoscale materials. The average particle size for each sample is provided in Table 3. Additionally, dynamic light scattering (DLS) measurements were used to determine the particle size with improved accuracy. The Z-average for each sample, representing the mean particle size, is also included in Table 3. These results underscore the consistent nanoscale dimensions of the ZnS particles (Table 4).

As shown in Table 3, the particle sizes measured by FESEM (primary particle size) are significantly smaller than the Z-average values obtained from DLS. For instance, ZnS4 exhibits an average FESEM particle size of approximately 35 nm, while its hydrodynamic diameter measured by DLS is about 187.4 nm. This discrepancy is expected and can be explained by the fundamental difference between the two techniques. FESEM directly visualizes and measures the dimensions of primary nanoparticles, whereas DLS measures the hydrodynamic diameter of particles in suspension, which includes contributions from agglomeration, surface-bound solvent molecules, and the electrical double layer. Therefore, the larger DLS values indicate that the synthesized ZnS nanoparticles tend to form agglomerates in solution, a common phenomenon for nanoscale materials due to van der Waals forces and high surface energy.

Table 3. FESEM images of ZnS nano-powders

Sample	Particle size (nm)*	Z-average (nm)
ZnS1	64	280.4
ZnS2	54	286.5
ZnS3	41	213.5
ZnS4	35	187.4
ZnS5	44	220.6
ZnS6	73	330.5
ZnS7	52	318.4
*Calculated from FESEM images by ImageJ software		

Table 4. Elemental composition of the ZnS samples

Sample	Zn(Wt.%)	S(Wt.%)	O(Wt.%)
ZnS1	62.98	32.81	4.21
ZnS2	63.01	32.93	4.06
ZnS3	63.11	33.96	2.93
ZnS4	64.12	33.32	2.56
ZnS5	62.73	31.54	4.73
ZnS6	62.59	32.21	5.20
ZnS7	62.71	32.10	5.19

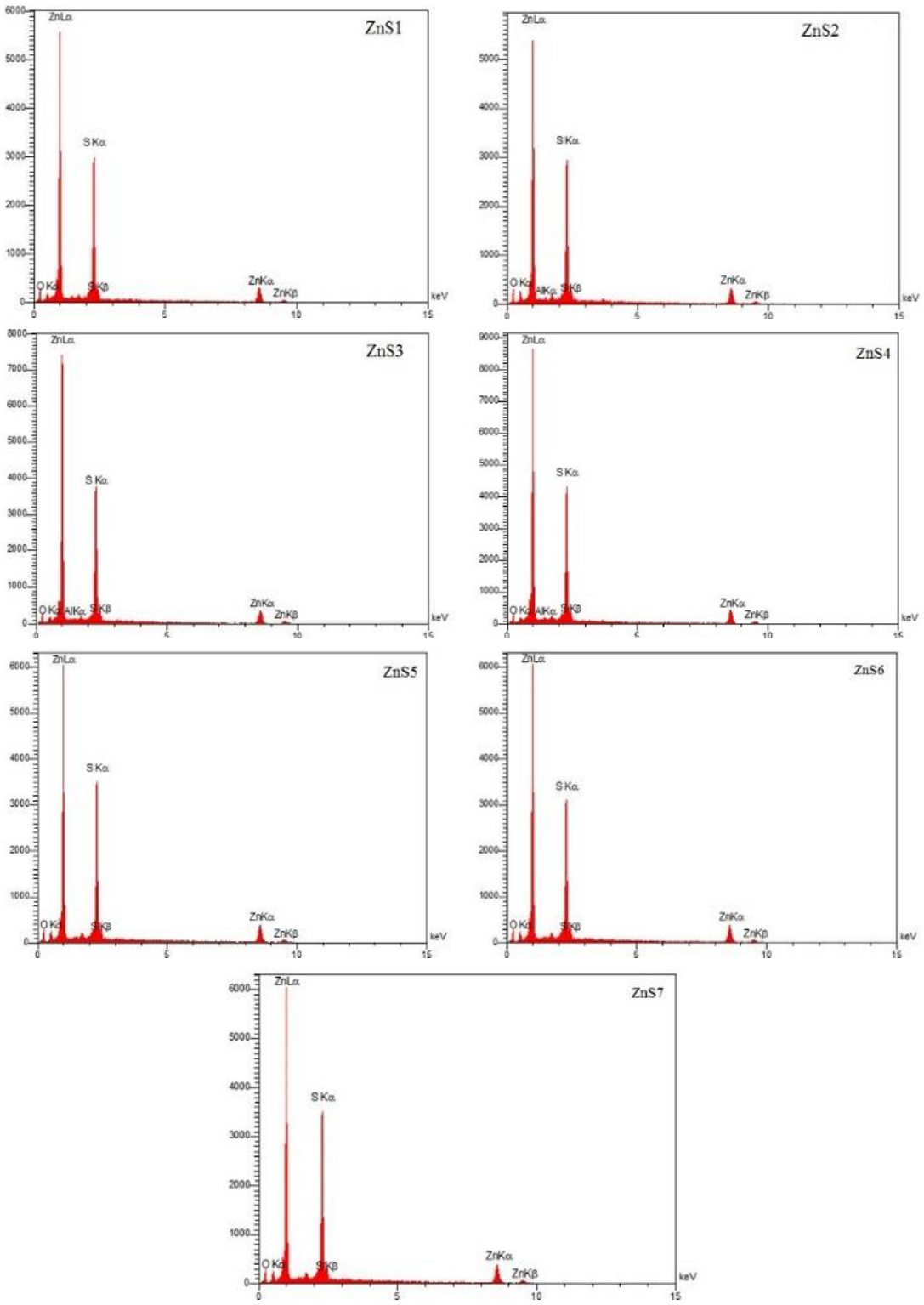

Figure 4. EDS images of ZnS nano-powders

3.2. Effect of synthesis parameters on ZnS nano-powders

3.2.1. Na_2S:$Zn(CH_3COO)_2$ ratio

This research examines the effects of altering the Na_2S to ($Zn(CH_3COO)_2$ ratio on the production of ZnS nanoparticles. The synthesis process was carried out at a constant temperature of 80°C and a pH of 4, utilizing three different weight ratios: 1.19:1, 1:1, and 2:1. The resulting samples were designated as ZnS1, ZnS2, and ZnS3, respectively.

The characterization results demonstrate that the ZnS nanoparticles produced with a 2:1 ratio (ZnS3) displayed broader and less intense peaks in the X-ray diffraction (XRD) pattern (Fig. 1) in comparison to the nanoparticles synthesized with the other two ratios (ZnS1 and ZnS2). This finding implies a reduced particle size for ZnS3, a conclusion that is further supported by the smaller crystallite size derived from the XRD data presented in Table 2.

FTIR spectroscopy analysis (Fig. 2) demonstrates that the ZnS3 sample exhibits a lower absorption edge in comparison to the ZnS1 and ZnS2 samples. This observation suggests a higher level of purity in the ZnS3 sample, indicating that the conditions under which it was synthesized were more effective in eliminating impurities. Furthermore, the observed increase in the ratio of sodium sulfide to zinc acetate seems to enhance the incorporation of sulfur into the ZnS synthesis process, thereby reducing the presence of free sulfur, which is considered a detrimental impurity in optical applications.

FESEM images (Fig. 3) reveal a reduction in the particle size of ZnS nanoparticles as the ratio of sodium sulfide to zinc acetate increases. The ZnS3 sample displays the smallest particle size, corroborating the findings from the X-ray Diffraction (XRD) and Fourier Transform Infrared FTIR spectroscopy analyses. This observation indicates that an elevated sodium sulfide ratio facilitates a greater dissolution of sulfide ions in the solution, thereby enhancing their incorporation during the synthesis of ZnS and ultimately yielding smaller nanoparticles [Yin, 2016; Viswanath, 2014].

The results of this study underscore the significant influence of the sodium sulfide to zinc acetate ratio on the size and purity of ZnS nanoparticles. A ratio of 2:1 is identified as optimal for the synthesis of smaller and purer nanoparticles, which may subsequently improve their optical properties and broaden their potential applications.

3.2.2. pH

This research investigates the influence of pH on the synthesis of ZnS nanoparticles, conducted at a constant temperature of 80 °C and utilizing a weight ratio of sodium sulfide to zinc acetate of 1.19:1. The samples were prepared at three distinct pH levels: 1.2, 4, and 5, which were subsequently designated as ZnS4, ZnS1, and ZnS5, respectively.

XRD analysis (Fig. 1) indicates that the ZnS sample produced at a pH of 1.2 (ZnS4) displays broader and less intense diffraction peaks in comparison with those of samples synthesized at pH 4 (ZnS1) and pH 5 (ZnS5). This observation implies that the ZnS4 sample possesses a smaller particle size. Furthermore, the crystallite size determined from the XRD data (Table 2) supports this conclusion, revealing a smaller crystallite size for the ZnS sample synthesized at pH 1.2.

FTIR spectroscopy analysis (Fig. 2) reveals a reduced absorption edge for the ZnS4 sample, which suggests a higher level of purity and more favorable synthesis conditions for the removal of impurities. This finding indicates that the increased acidity of the zinc acetate solution at lower pH levels enhances the reactivity of hydrogen ions with free species present in the synthesis environment. As a result, these impurities are more efficiently removed during the drying and washing processes.

FESEM images (Fig. 3) indicate a reduction in the size of ZnS nanoparticles as the pH decreases. The increased concentration of hydrogen ions at lower pH levels may facilitate the adsorption of these ions onto the surface of zinc sulfide particles, thereby generating electrostatic repulsion among them. This repulsive interaction may inhibit particle flocculation in the solution, ultimately resulting in smaller particle dimensions.

These observations suggest that pH is a critical factor influencing both the size and purity of ZnS nanoparticles. Specifically, lower pH values appear to enhance the removal of impurities and contribute to the formation of smaller particle sizes.

3.2.3. Temperature

The objective of this study was to clarify the influence of temperature on the synthesis of ZnS nanoparticles while keeping the pH constant at 4 and maintaining a fixed weight ratio of sodium sulfide to zinc acetate at 1.19:1. Three different temperatures were used in the experiments: 50 °C, 80 °C, and 100 °C, leading to the designation of the resulting samples as ZnS1, ZnS6, and ZnS7, respectively.

XRD analysis (Fig. 1) demonstrated the presence of consistent characteristic peaks across the synthesized samples, indicating that temperature variations did not induce significant structural changes. Nevertheless, the sample synthesized at 100 °C (ZnS7) displayed a decrease in crystallite size compared with the samples ZnS1 and ZnS6.

FTIR spectroscopy (Fig. 2) demonstrated a reduced intensity of the water-related band in the spectrum of ZnS1 compared with those of ZnS6 and ZnS7. This finding suggests lower moisture content in ZnS1, which may indicate a more effective dehydration process occurring at lower temperatures.

FESEM images (Fig. 3) revealed a clear trend indicating a reduction in particle size as the temperature

increased. The ZnS7 sample displayed the smallest particle size compared with ZnS1 and ZnS6, thereby supporting the assertion that higher synthesis temperatures promote the formation of smaller ZnS nanoparticles. Collectively, these results suggest that temperature significantly affects the size of synthesized ZnS nanoparticles, with elevated temperatures promoting the formation of smaller particles while preserving a uniform crystallographic structure.

3.2. Characterizations of sintered ZnS

The ZnS4 sample was selected and subjected to sintering via the spark plasma sintering technique. Figure 5 displays the X-ray diffraction pattern of the sintered ZnS4. It is evident that the sample comprises two dominant phases: hexagonal (reference code: 01-089-2194) and cubic (reference code: 01-077-2100). The figure shows a decrease in peak width and an increase in peak intensity, phenomena that can be attributed to grain growth occurring during the SPS process. The crystallite size of the synthesized ZnS powder was estimated using the Scherrer equation to be approximately 40 nm; however, following sintering, the crystallite size increased to over 110 nm. Importantly, peaks associated with free sulfur were not observed in the XRD analysis of the ZnS4 powder; nonetheless, these peaks became detectable in the sintered sample, suggesting the presence of sulfur as a consequence of grain growth during sintering.

The transmittance spectrum of the synthesized ZnS ceramic, recorded at ambient temperature over the range of 2.5 to 25 µm, is illustrated in Figure 6. The spectrum reveals a transmittance of approximately 30% within the 8–12 µm infrared region, which is often designated as the atmospheric window. This finding suggests that the ZnS ceramic exhibits significant transparency to infrared radiation within this wavelength range. Such a property is particularly relevant for applications requiring the transmission of infrared radiation, including infrared detectors, optical fibers, and thermal imaging systems.

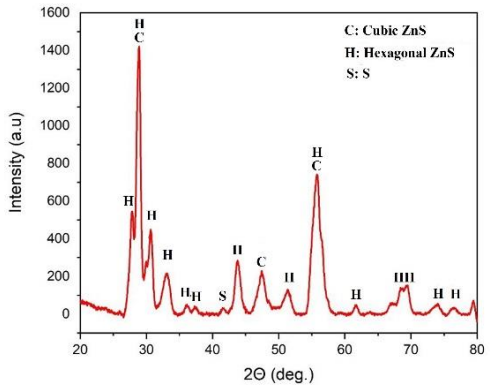

Figure 5. XRD pattern of sintered ZnS4 nano-powder by SPS method

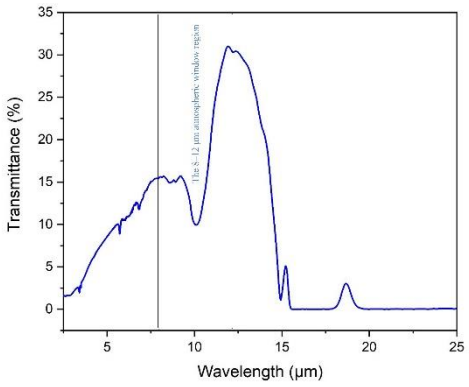

Figure 6. FTIR transmission of ZnS4 ceramic processed by SPS

4. CONCLUSIONS

In this study, zinc sulfide nanopowder was synthesized through a chemical synthesis method. The influence of various synthesis parameters, including the mass ratio of the sulfide source to the zinc source, the pH of the solution, and the synthesis temperature, was systematically examined. The analysis indicated that the nanopowder produced at a pH of 1.2 (ZnS4) exhibited an average particle size of 31 nm, which was notably smaller than that of the other synthesized nanopowders. The purity of the synthesized material was confirmed by FTIR analysis, which revealed a lower level of impurities and a reduced absorption edge compared with other samples. In addition, the sintered ZnS4 sample demonstrated a transmittance of approximately 30% within the infrared wavelength range of 8–12 µm, highlighting its potential applicability in optical domains such as infrared windows or coatings.

ACKNOWLEDGEMENTS

This research work has been supported with research grant (No.: 413124) by Materials and Energy Research Center (MERC), Karaj, Iran.

References

1. Abedi, M., et al., *An analytical review on Spark Plasma Sintering of metals and alloys: From processing window, phase transformation, and property perspective.* Critical reviews in solid state and materials sciences, 2023. **48**(2): p. 169-214. https://doi.org/10.1080/10408436.2022.2049441

2. Chen, Y., et al., *Fabrication of transparent ZnS ceramic by optimizing the heating rate in spark plasma sintering process.* Optical Materials, 2015. **50**: p. 36-39. https://doi.org/10.1016/j.optmat.2015.03.058

3. Drezner, Y., S. Berger, and M. Hefetz, *A correlation between microstructure, composition and optical transparency of CVD-ZnS.* Materials Science and Engineering: B, 2001. **87**(1): p. 59-65. https://doi.org/10.1016/S0921-5107(01)00701-2

4. Li, Y. and Y. Wu, *Transparent and luminescent ZnS ceramics consolidated by vacuum hot pressing method.* Journal of the American Ceramic Society, 2015. **98**(10): p. 2972-2975. https://doi.org/10.1111/jace.13781

5. Li, Y., et al., *Hot-pressed chromium doped zinc sulfide infrared transparent ceramics.* Scripta Materialia, 2016. **125**: p. 15-18. https://doi.org/10.1016/j.scriptamat.2016.07.027

6. Ramavath, P., et al., *Effect of sphalerite to wurtzite crystallographic transformation on microstructure, optical and mechanical properties of zinc sulphide ceramics.* Ceramics International, 2011. **37**(3): p. 1039-1046. https://doi.org/10.1016/j.ceramint.2010.11.032

7. Ramavath, P., et al., *Hot isostatic pressing of ZnS powder and CVD ZnS ceramics: comparative evaluation of physico-chemical, microstructural and transmission properties.* Transactions of the Indian Ceramic Society, 2014. **73**(4): p. 299-302. https://doi.org/10.1080/0371750X.2014.931252

8. Rema Devi, B., R. Raveendran, and A. Vaidyan, *Synthesis and characterization of Mn2+-doped ZnS nanoparticles.* Pramana, 2007. **68**(4): p. 679-687. https://doi.org/10.1007/s12043-007-0068-7

9. Sharma, A. and G. Oza, *Synthesis, Characterization and Applications. 2023* https://www.amazon.com/dp/B0BRP7S8WL

10. Viswanath, R., et al., *Studies on characterization, optical absorption, and photoluminescence of yttrium doped ZnS nanoparticles.* Journal of Nanotechnology, 2014. **2014**(1): p. 924797. https://doi.org/10.1155/2014/924797

11. Yashina, E., E. Gavrishchuk, and V. Ikonnikov, *Mechanisms of polycrystalline CVD ZnS densification during hot isostatic pressing.* Inorganic materials, 2004. **40**: p. 901-904. https://doi.org/10.1023/B:INMA.0000041317.61466.d6

12. Yeo, S.-Y., et al., *Sintering and optical properties of transparent ZnS ceramics by pre-heating treatment temperature.* Journal of Electroceramics, 2018. **41**: p. 1-8. https://doi.org/10.1007/s10832-018-0137-y

13. Yin, L., et al., *Morphology-controllable synthesis and enhanced photocatalytic activity of ZnS nanoparticles.* Journal of Alloys and Compounds, 2016. **664**: p. 476-480. https://doi.org/10.1016/j.jallcom.2015.10.281

14. Zahabi, S., et al., *Effect of H2S gas flow rate on the stoichiometric ratio of S: Zn and transparency of ZnS nanostructure ceramic in IR region.* Ceramics International, 2024. **50**(11): p. 20706-20717. https://doi.org/10.1016/j.ceramint.2024.03.192